Investigation of the relevant kinetic processes in the initial stage of a double-arcing instability in oxygen plasmas

B. Mancinelli, L. Prevosto, J. C. Chamorro, F. O. Minotti, and H. Kelly

Citation: Physics of Plasmas **25**, 054504 (2018); doi: 10.1063/1.5032220
View online: https://doi.org/10.1063/1.5032220
View Table of Contents: http://aip.scitation.org/toc/php/25/5
Published by the American Institute of Physics

Investigation of the relevant kinetic processes in the initial stage of a double-arcing instability in oxygen plasmas

B. Mancinelli,[1] L. Prevosto,[2,a)] J. C. Chamorro,[1] F. O. Minotti,[3,4] and H. Kelly[1]
[1]*Grupo de Descargas Eléctricas, Departamento Ing. Electromecánica, Facultad Regional Venado Tuerto (UTN), Laprida 651, Venado Tuerto 2600, Santa Fe, Argentina*
[2]*Universidad Tecnológica Nacional, CONICET, Facultad Regional Venado Tuerto Departamento Ing. Electromecánica, Grupo de Descargas Eléctricas, Laprida 651, Venado Tuerto 2600, Santa Fe, Argentina*
[3]*Universidad de Buenos Aires, Facultad de Ciencias Exactas y Naturales, Departamento de Física, Buenos Aires 1428, Argentina*
[4]*CONICET-Universidad de Buenos Aires, Instituto de Física del Plasma (INFIP), Buenos Aires 1428, Argentina*

(Received 3 April 2018; accepted 25 April 2018; published online 11 May 2018)

A numerical investigation of the kinetic processes in the initial (nanosecond range) stage of the double-arcing instability was developed. The plasma-sheath boundary region of an oxygen-operated cutting torch was considered. The energy balance and chemistry processes in the discharge were described. It is shown that the double-arcing instability is a sudden transition from a diffuse (glow-like) discharge to a constricted (arc-like) discharge in the plasma-sheath boundary region arising from a field-emission instability. A critical electric field value of $\sim 10^7$ V/m was found at the cathodic part of the nozzle wall under the conditions considered. The field-emission instability drives in turn a fast electronic-to-translational energy relaxation mechanism, giving rise to a very fast gas heating rate of at least $\sim 10^9$ K/s, mainly due to reactions of preliminary dissociation of oxygen molecules via the highly excited electronic state $O_2(B^3\Sigma_u^-)$ populated by electron impact. It is expected that this fast oxygen heating rate further stimulates the discharge contraction through the thermal instability mechanism. *Published by AIP Publishing.*
https://doi.org/10.1063/1.5032220

Plasma cutting is a widely extended process of metal cutting at atmospheric pressure by an arc plasma jet.[1] In order to obtain a "high-energy density" plasma flow, a plasma jet (oxygen is usually used as plasma gas) carrying a low-current (~30 to 100 A) is forced to flow through a small orifice (~1 mm) of an electrically neutral (floating) nozzle. One of the most significant drawbacks of this process is the so-called "double-arcing" phenomenon, which is a type of plasma instability inherent to the arc stabilization method.[2] A small loop current circulating through the nozzle body (resembling a unipolar discharge[3]) is a feature of this mode of arc stabilization due to the floating nozzle being in contact with the regions of plasma with differing characteristics (the arc voltage drop inside the nozzle is much higher than the electron temperature[2]). One part of the nozzle collects electrons while the other part collects ions. The compensation between the ionic and electronic currents requires that the nozzle potential be close to that of the arc at the nozzle inlet[4] (i.e., the total arc voltage drop inside the nozzle is close to the voltage drop across the plasma-sheath boundary region at the nozzle exit). With increased applied fields (as, for instance, for a too large arc current[2]), an instability mechanism comes into operation in the plasma-sheath boundary region at the nozzle exit as a chain of causal processes (onset of additional kinetic processes and locally increased ionization, movement of the new ions to the nozzle wall, and the creation of a new cathode spot attachment by ion impact), and ultimately a constricted-type discharge carrying a substantial part of the arc current (i.e., a double-arcing) flows through the floating nozzle, likely destroying it.[2] Experimental results show that depending on specific conditions, the characteristic instability time could vary from 10^{-6} to 10^{-4} s.[5,6]

Despite the great interest and practical importance for the cutting process, only a few papers[5–8] were dedicated to explore the double-arcing. Although there are some differences in the conclusions of those works, all coincide in that the double-arcing results from a high voltage drop inside the nozzle. However, the understanding of what specific mechanism triggers the double-arcing phenomenon is less clear. At present, there is no self-consistent theoretical model describing the gas heating and charged particles kinetic processes of the mechanism of the double-arcing development. Note that gas heating is one of the main issues in the theory of gas breakdown because as the gas temperature increases additional ionization processes come into play. The development of such a model is the main purpose of this work.

A numerical investigation of the initial stage of the double-arcing phenomena with the focus on the kinetic processes is presented. This work is based on a previously reported fluid model,[4] which was used there to describe the properties of the unipolar-like, diffuse discharge in the plasma-sheath boundary region of a cutting arc torch operated with oxygen (Fig. 1). Note that the conditions studied in that work are those corresponding to the normal operation of the torch (i.e., prior to double-arcing, where most of the

a)Author to whom correspondence should be addressed: prevosto@waycom.com.ar

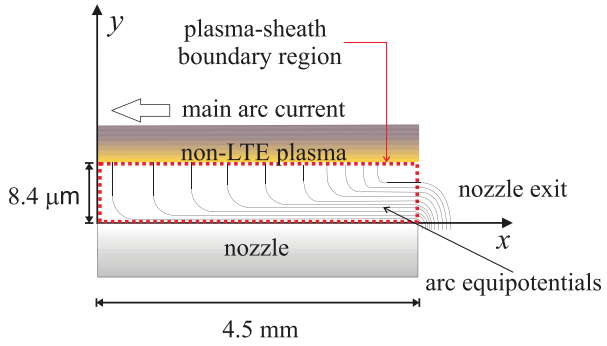

FIG. 1. The scheme of the plasma-sheath boundary region (x and y being the axial and normal to the nozzle wall coordinates, respectively).

current flows through the arc core) and not the double-arcing conditions, the case this work is dedicated to.

In spite of the 3D nature of the double-arcing, a 2D approach is used in the present work. In the case of 3D models, the complexity associated with a detailed kinetic model increases enormously. However, a 2D model can still give useful information about the kinetic processes in the initial (nanosecond range) stage of the discharge contraction because 3D (azimuthal) effects are not yet developed.

The model considers a fairly complete set of 45 chemical reactions and processes with the participation of 12 oxygen species [O^+, O_2^+, O_4^+, O_2^-, $O_2(a^1\Delta_g)$, $O_2(A^3\Sigma_u^+)$, $O_2(B^3\Sigma_u^-)$, $O_2(9.97\,\text{eV})$, $O(^1D)$, $O(^1S)$, $O(^3P)$, and $O_2(X^3\Sigma_g^-)$] and electrons (e), describing the energy balance and charged particle kinetic processes in the discharge. The set of reactions used and related rate coefficients were presented in Table I of Ref. 4. The electron transport and source parameters were calculated using the Bolsig+[9] as functions of the mean electron energy. The model takes into account the previously suggested mechanisms[10] to describe observations of fast gas heating in moderate ($\sim 10^2$ Td; being $1\,\text{Td} \equiv 10^{-21}\,\text{V m}^2$) reduced electric fields, as well as the processes that become important in the presence of high electric fields (>500 Td),[11] and also includes the mechanisms of energy release in direct and stepwise dissociative ionization of the oxygen. More details on the equations of the model and the treatment of the transport and source terms can be found in Ref. 4.

In particular, the following processes responsible for the gas temperature increase are relevant under the present conditions: the dissociation of oxygen molecules [reactions (R4)–(R6) in Table I of Ref. 4] by electron-impact following predissociation from electronically excited states (e.g. Ref. 12)

$$\begin{aligned}
&e + O_2\left(X^3\Sigma_g^-\right) \rightarrow e + O_2\left(A^3\Sigma_u^+\right),\\
&O_2\left(A^3\Sigma_u^+\right) \rightarrow O(^3P) + O(^3P) + 0.8\,\text{eV},\\
&e + O_2\left(X^3\Sigma_g^-\right) \rightarrow e + O_2\left(B^3\Sigma_u^-\right),\\
&O_2\left(B^3\Sigma_u^-\right) \rightarrow O(^3P) + O(^1D) + 1.26\,\text{eV},\\
&e + O_2\left(X^3\Sigma_g^-\right) \rightarrow e + O_2(9.97\,\text{eV}),\\
&O_2(9.97\,\text{eV}) \rightarrow O(^3P) + O(^1S) + 0.6\,\text{eV}, \qquad (1)
\end{aligned}$$

and the dissociative ionization of $O_2(X^3\Sigma_g^-)$ [reaction (R9) in Table I of Ref. 4] and from the metastable state $O_2(a^1\Delta_g)$ [reaction (R10) in Table I of Ref. 4]. The products O^+ can have significant kinetic energy ~3 eV (Ref. 13)

$$\begin{aligned}
&e + O_2\left(X^3\Sigma_g^-\right) \rightarrow e + e + O^+ + O(^3P) + 3\,\text{eV},\\
&e + O_2\left(a^1\Delta_g\right) \rightarrow e + e + O^+ + O(^3P) + 3\,\text{eV}. \qquad (2)
\end{aligned}$$

The boundary conditions for the model equations correspond in general to the conditions in Ref. 4. At the sheath-plasma interface, axial profiles of plasma and gas densities as well as the electron temperature were specified as constant in time, thus imposing restrictions on the discharge time. Note that to find the precise boundary conditions it would be necessary to solve the entire discharge problem self-consistently, which is beyond the scope of this work. The electron emission from the nozzle wall incorporates the ion-enhanced field emission on the basis of the Fowler–Nordheim equation.[14] The electrostatic potential at the nozzle wall was self-consistently calculated by using the total current (conduction plus displacement) conservation throughout the nozzle surface. In the calculations, the following parameters were assumed: $\gamma_0 = 0.13$,[15] $\phi = 2$ eV (for an oxidizing copper surface),[16] and $\beta \sim 100$.[17] (γ_0 is the ion-induced secondary electron emission coefficient for zero electric field, ϕ is the work function, and β is the geometric enhancement factor of the local electric field at the wall).

The model equations were solved using the same numerical scheme as reported in Ref. 4. A uniform rectangular grid with 20×20 mesh cells covered the rectangular model geometry. To avoid numerical instabilities, a temporal step shorter than 1×10^{-13} s was used.

The double-arcing development was initiated by perturbing the diffuse discharge in the plasma-sheath boundary,[4] by a local rise in the surface electric field over a small area of the nozzle exit. Actually, such increase in the electric field can be associated with a change in the surface microstructure,[17] or the deposition of non-conducting films[7] on the nozzle wall. It was found that a slight increase in the value of the geometric enhancement factor β (from 95 to about 114) gives rise to a double-arcing instability under the studied conditions. However, for lower values of β the perturbation decayed in a time of a few nanoseconds. In order to approximately sustain the boundary conditions at the plasma-sheath interface, the discharge time was restricted to the first nanoseconds (0–7 ns) of the instability.

Figure 2 shows the calculated distributions of electrons and positive ions (representing the concentration of O_2^+ plus O^+) at different times and illustrates the dynamics of the contraction of the discharge during the initial stage of the double-arcing phenomenon. The initial charged particle densities correspond to the stationary solution of the model presented in Ref. 4.

By comparing Figs. 2(b) and 2(d), it is evident that a large positive space-charge appears in the vicinities of the wall at the nozzle exit (i.e., at the cathodic part) during the discharge contraction. The formation of this space-charge is induced by the ion-enhanced field emission from the wall through further ionization of $O_2(X^3\Sigma_g^-)$, mainly in reaction (R7) in Table I of Ref. 4 although a non-negligibly

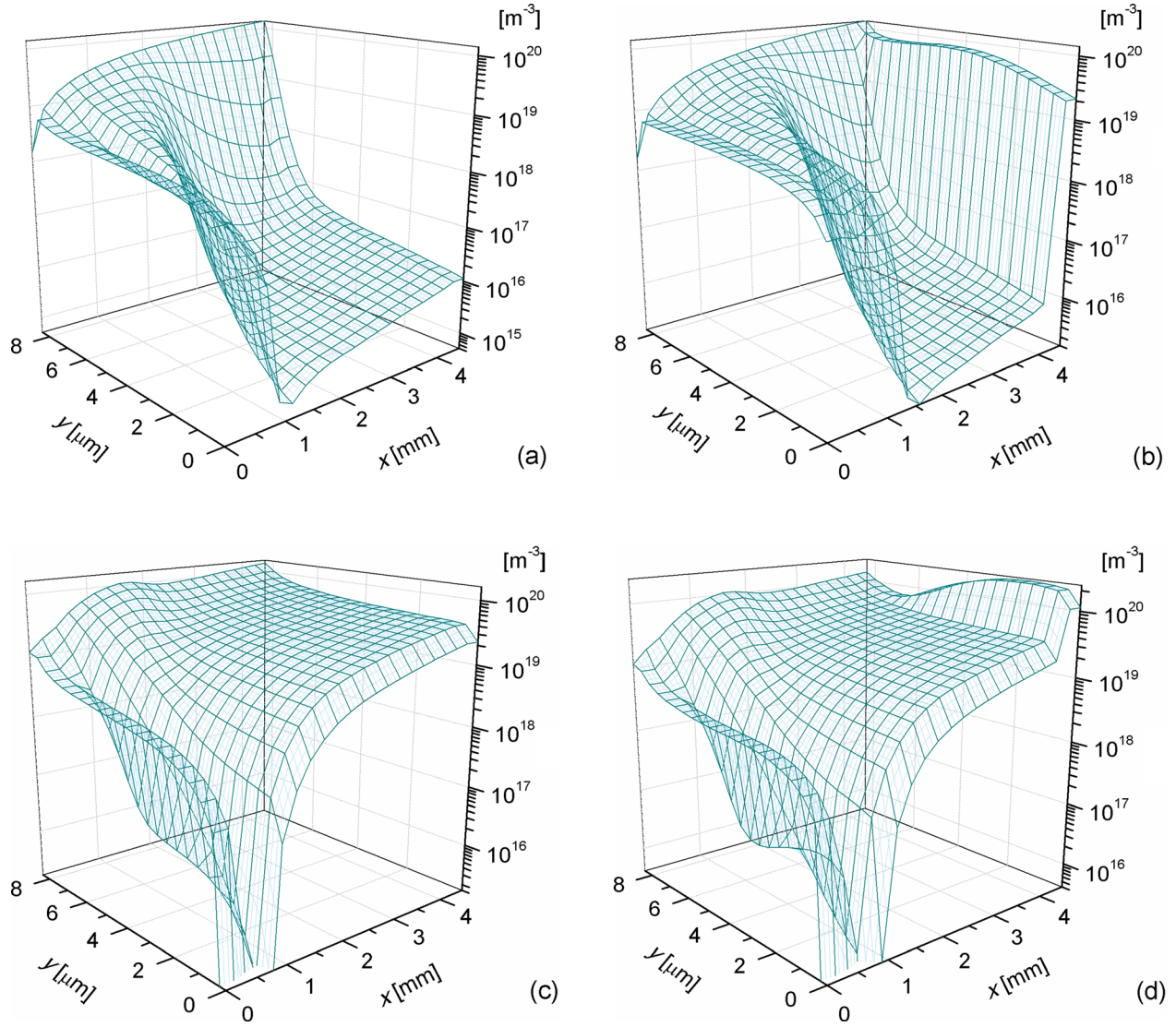

FIG. 2. 2D number density profiles corresponding to different times: electrons at $t = 0$ s (a) and at $t = 7$ ns (b); positive ions at $t = 0$ s (c) and at $t = 7$ ns (d).

concentration of O^+ also occurs in that location, mainly due to the dissociative ionization of $O_2(X^3\Sigma_g^-)$ [reaction (R9) in Table I of Ref. 4]. Such a space-charge is responsible for the establishment of the local high-electric field strength at the cathode of the discharge.

Because of the large field at the cathode, the emitted electrons from the wall produce further ionization processes. The positive ions from these processes in turn increase the local electric field by their space-charge. This increased field at the cathode enhances the electron field emission and a sudden transition from a diffuse (glow-like) discharge to a constricted (arc-like) discharge arises.[18] This "field-emission instability" mechanism is illustrated in Fig. 3, where the temporal evolution of the electric field and the electron current density (in absolute value) at the cathode are shown. Once the ionization of neutrals starts, the positive space-charge

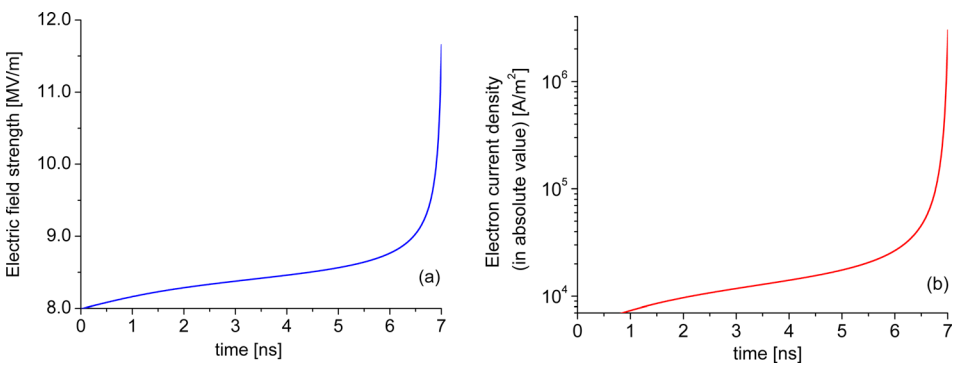

FIG. 3. Temporal evolution of the sheath properties at the cathode of the discharge: electric field strength (a) and electron current density in absolute value (b).

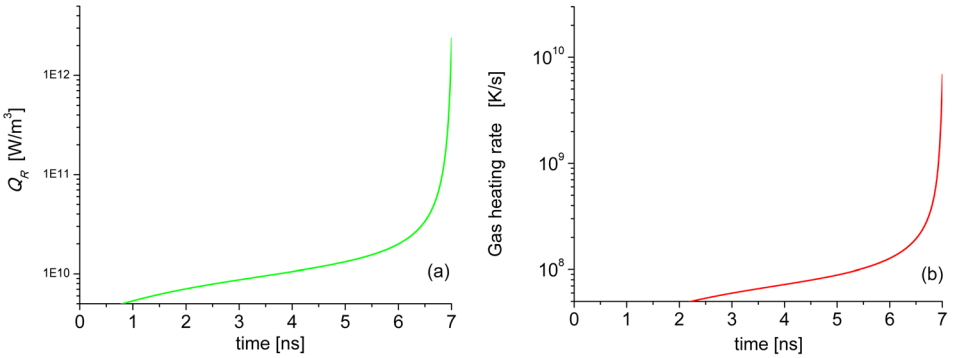

FIG. 4. Temporal evolution of the sheath properties at the cathode of the discharge: gas power deposition due to chemical reactions (a) and gas heating rate (b).

increases, ultimately producing an exponential increase in both the electric field and current density with time when the field at the cathode reaches a critical value of $\sim 10^7$ V/m under the considered conditions. However, it is important to note that small differences either in the work function or in the surface roughness can modify the calculated critical value. The dynamics at the cathode also produces an increase in the nozzle voltage ($\sim$1 V after 7 ns), which in turn allows more electrons to return to the wall at the nozzle inlet (i.e., at the anodic part). The return flow of electrons as well as the displacement current closes the current loop ($\sim$1 A after 7 ns) of the discharge.

The temporal evolution of the gas power deposition term Q_R due to the electronic-to-translational energy relaxation mechanism and the gas heating rate calculated at the cathode of the discharge is shown in Fig. 4. The gas is heated mainly in the reactions of preliminary dissociation of highly excited electronic states of $O_2(X^3\Sigma_g^-)$ that are produced by electron impact [Eq. (1)]. About 65% of the power spent on gas heating is produced by the dissociation of $O_2(X^3\Sigma_g^-)$ into $O(^3P) + O(^1D)$ via the excited states $O_2(B^3\Sigma_u^-)$. The dissociative ionization of O_2 $(X^3\Sigma_g^-)$ [Eq. (2)] contributes to about 30% of the power spent on gas heating; the higher the mean electron energy, the larger the role of the latter process. The fractions of the electron power (about 96 W after 7 ns) spent on dissociation and ionization of oxygen are about 46% and 29%, respectively, while the fraction of the power spent on electronic excitation and further converted to fast gas heating is about 12%. By comparing the current results with those presented in Ref. 4, large changes in the contribution of the exothermic processes to the balance of the gas heating in the discharge are evident due to the enhancement of the electron-impact excitation processes. Prior to double-arcing, a large part (about 63%) of the power spent on gas heating is produced by ion-molecule and recombination reactions and by the electron attachment. The electron power deposited on the bulk of the sheath is less than 0.5 W (most of the electron population is repelled in front of the nozzle wall) and only a fraction of it, about 25%, is locally consumed in electron-impact excitation processes.

Note from Fig. 4 that the oxygen gas is heated at a very fast rate of at least 10^9 K/s during the instability development due to the fast electronic-to-translational relaxation energy rate at strong gas excitation conditions [$n_e \sim 10^{19}$ m^{-3}, Fig. 2(b)]. Such a fast gas heating rate is comparable to that that occurs in the head of a leader propagating in air.[10] Recently, an ultrafast gas heating rate of 5×10^{10} K/s has been reported in a nanosecond pulsed discharge in atmospheric pressure air.[19] The main heating mechanism was identified as the fast electronic energy relaxation in reactions of preliminary dissociation of oxygen molecules through the quenching reaction of the $N_2(B^3\Pi_g)$. It is expected that the fast oxygen heating rate in the plasma-sheath boundary further stimulates the discharge contraction through the thermal instability mechanism.[16]

In conclusion, a 2D self-consistent model was for the first time reported of the time-resolved dynamics of the initial stage (nanosecond range) of the double-arcing phenomena, with the focus on the kinetic processes leading to the fast gas heating during the discharge contraction. This model extends our previous work[4] developed to describe the properties of the diffuse (unipolar-like) discharge that occurs prior to double-arcing phenomenon in the plasma-sheath boundary region of an oxygen-operated cutting arc. In particular, the results of the model show the following:

(1) The double-arcing instability is a sudden transition from a diffuse (glow-like) discharge to a constricted (arc-like) discharge in the plasma-sheath boundary region arising from a field-emission instability. A critical electric field value of $\sim 10^7$ V/m was found at the cathodic part of the nozzle wall under the conditions considered.
(2) The field-emission instability drives in turn a fast electronic-to-translational energy relaxation mechanism, giving rise to a very fast gas heating rate of at least $\sim 10^9$ K/s, mainly due to reactions of preliminary dissociation of oxygen molecules via the highly excited electronic state $O_2(B^3\Sigma_u^-)$ populated by electron impact. It is expected that the fast oxygen heating rate further stimulates the discharge contraction through the thermal instability mechanism.

This work was supported by the grants from the CONICET (PIP 11220120100453) and Universidad Tecnológica Nacional (PID 4626). L.P. and F.O.M. are members of the CONICET. J.C.C. thanks CONICET for his doctoral fellowships.

[1]M. Boulos, P. Fauchais, and E. Pfender, *Thermal Plasmas, Fundamentals and Applications* (Plenum Press, New York and London, 1994), Vol. 1.
[2]V. A. Nemchinsky and W. S. Severance, J. Phys. D: Appl. Phys. **39**, R423 (2006).

[3]H. J. G. Gielen and D. C. Schram, IEEE Trans. Plasma Sci. **18**, 127 (1990).
[4]B. Mancinelli, L. Prevosto, J. C. Chamorro, F. O. Minotti, and H. Kelly, Plasma Chem. Plasma Process. **38**, 147 (2018).
[5]L. Prevosto, H. Kelly, and B. Mancinelli, J. Appl. Phys. **105**, 013309 (2009).
[6]L. Prevosto, H. Kelly, and B. Mancinelli, J. Appl. Phys. **110**, 083302 (2011).
[7]V. A. Nemchinsky, J. Phys. D: Appl. Phys. **42**, 205209 (2009).
[8]B. Mancinelli, F. O. Minotti, L. Prevosto, and H. Kelly, J. Appl. Phys. **116**, 023301 (2014).
[9]G. J. M. Hagelaar and L. C. Pitchford, Plasma Sources Sci. Technol. **14**, 722 (2005).
[10]N. A. Popov, Plasma Phys. Rep. **27**, 886 (2001).
[11]N. L. Aleksandrov, S. V. Kindysheva, M. M. Nudnova, and A. Yu. Starikovskiy, J. Phys. D: Appl. Phys. **43**, 255201 (2010).
[12]C. D. Pintassilgo and V. Guerra, Plasma Sources Sci. Technol. **24**, 055009 (2015).
[13]M. Capitelli and J. N. Bardsley, *Non-Equilibrium Processes in Partially Ionized Gases* (Plenum Press, New York, 1989).
[14]D. B. Go and D. A. Pohlman, J. Appl. Phys. **107**, 103303 (2010).
[15]H. Hannesdottir and J. T. Gudmundsson, Plasma Sources Sci. Technol. **25**, 055002 (2016).
[16]Y. P. Raizer, *Gas Discharge Physics* (Springer, Berlin, 1991).
[17]Z. Insepov and J. Norem, J. Vac. Sci. Technol. A **31**, 011302 (2013).
[18]W. S. Boyle and F. E. Haworth, Phys. Rev. **101**, 935 (1956).
[19]D. L. Rusterholtz, D. A. Lacoste, G. D. Stancu, D. Z. Paiand, and C. O. Laux, J. Phys. D: Appl. Phys. **46**, 464010 (2013).